Edge Time Series Components of Functional Connectivity and Cognitive Function in Alzheimer's Disease

Evgeny J. Chumin[1,2,3,4,*], Sarah A. Cutts[1,5], Shannon L. Risacher[2,3,4,6], Liana G. Apostolova[2,3,4,6,7], Martin R. Farlow[3,4,7], Brenna C. McDonald[2,3,4,6,7], Yu-Chien Wu[3,4,6], Richard Betzel[1,2,5], Andrew J. Saykin[2,3,4,6,7], Olaf Sporns[1,2,3,4,5,6]

1 Department of Psychological and Brain Sciences, Indiana University (IU), Bloomington, IN, United States
2 Indiana University Network Sciences Institute, IU, Bloomington, IN, United States
3 Stark Neurosciences Research Institute, Indiana University School of Medicine (IUSM), Indianapolis, IN, United States
4 Indiana Alzheimer's Disease Research Center, IUSM, Indianapolis, IN, United States
5 Program in Neuroscience, IU, Bloomington, IN, United States
6 Department of Radiology and Imaging Sciences, IUSM, Indianapolis, IN, United States
7 Department of Neurology, IUSM, Indianapolis, IN, United States

Abstract

Understanding the interrelationships of brain function as measured by resting-state magnetic resonance imaging and neuropsychological/behavioral measures in Alzheimer's disease is key for advancement of neuroimaging analysis methods in clinical research. The edge time-series framework recently developed in the field of network neuroscience, in combination with other network science methods, allows for investigations of brain-behavior relationships that are not possible with conventional functional connectivity methods. Data from the Indiana Alzheimer's Disease Research Center sample (53 cognitively normal control, 47 subjective cognitive decline, 32 mild cognitive impairment, and 20 Alzheimer's disease participants) were used to investigate relationships between functional connectivity components, each derived from a subset of time points based on co-fluctuation of regional signals, and measures of domain-specific neuropsychological functions. Multiple relationships were identified with the component approach that were not found with conventional functional connectivity. These involved attentional, limbic, frontoparietal, and default mode systems and their interactions, which were shown to couple with cognitive, executive, language, and attention neuropsychological domains. Additionally, overlapping results were obtained with two different statistical strategies (network contingency correlation analysis and network-based statistics correlation). Results demonstrate that connectivity components derived from edge time-series based on co-fluctuation reveal disease-relevant relationships not observed with conventional static functional connectivity.

Keywords

Functional connectivity, Alzheimer's disease, brain networks, brain-behavior relationships

Corresponding Author

Evgeny J. Chumin, Psychology Building 308, 1101 E 10th St, Bloomington, IN, 47405, United States
E-mail address: echumin@iu.edu

Introduction

Various neuroimaging modalities can now capture multiple facets of Alzheimer's disease (AD), offering tools for characterization and understanding of disease impacts on brain and cognitive functions. Such understanding is important as over 6 million people are affected by AD in United States alone, a number that is projected to rise to over 12 million by 2050 according to the 2022 Alzheimer's Association Annual Report. Pathological hallmarks of AD, beta-amyloid plaques and hyperphosphorylated tau tangles, have been imaged *in vivo* with positron emission tomography, showing increasing accumulation of both as disease severity progresses (Therriault et al. 2022). Accumulation of tau and its spread have also been shown to occur within the functional network organization of the brain (Franzmeier et al. 2020; Franzmeier et al. 2019). These networks were identified in early functional magnetic resonance imaging (fMRI) studies of task-based and resting-state connectivity (Buckner et al. 2008; Fox et al. 2006; Yeo et al. 2011). Since then, numerous fMRI studies in AD have reported alterations in the properties of resting state networks (RSNs) such as their strength (Dai et al. 2019; Dai et al. 2015) and interconnectivity (Forouzannezhad et al. 2019). Changes in these network properties have also been related to cognitive function (Chumin et al. 2021; Contreras et al. 2019) and existing biomarkers (Smith et al. 2021; Veitch et al. 2019).

In recent years, in parallel with the improvement in the temporal resolution of fMRI, studies of the temporal dynamics of the brain and its RSNs have emerged (Hutchison et al. 2013; Lurie et al. 2020). Even over the relatively short duration of a typical fMRI scan, brain functional networks exhibit significant dynamic fluctuations, and this observation raises the question whether time points differentially contribute/relate to neuropsychological outcomes of interest. This is supported by literature investigating brain states, where clustering algorithms were used to group functional connectivity (FC) patterns of activity (Calhoun et al. 2014; Cohen 2018). AD-related alterations in the dynamics of FC are marked by reduced internetwork connectivity (Schumacher et al. 2019), which is related to cognitive function (Franzmeier et al. 2017). Additionally, the emergence and duration of these states, as well as the transition between them, has been shown to be different in AD relative to other diagnostic groups (Schumacher et al. 2019). Such methods divide the data into non- or partially overlapping temporally continuous subsets (windows) to study FC-cognition relationships in AD. However, over the duration of a resting-state scan, it is likely that individual time points differentially relate to neurocognitive outcomes and behaviors. In this case, methods that assess functional properties at single repetition time (TR, a single fMRI time point) resolution are better suited to probe these relationships. To date, no methods have been employed in clinical AD that probe brain-behavior at single-TR resolution.

A method to probe single-TR connectivity dynamics has recently been proposed by Faskowitz et al. (2020), which relies on 'temporal unwrapping' of the Pearson correlation conventionally used to estimate FC, to yield moment-to-moment co-fluctuations. Computed as the elementwise product of regional blood-oxygen-level-dependent (BOLD) signals, co-fluctuations are represented as an edge (connection) by time matrix of edge time-series (ETS). This approach offers an intuitive interpretation of the ongoing dynamics in the brain and has been employed to probe modular/community structure (Faskowitz et al. 2020; Jo et al. 2021), individual variability (Betzel et al. 2022; Cutts et al. 2022; Sasse et al. 2022), and disease-related alterations in brain function (Idesis et al. 2022; Zamani Esfahlani et al. 2022). Previous work on ETS in young healthy individuals from the Human Connectome Project (Van Essen et al. 2013) dataset has shown that FC can be approximated from a subset of scan time points with highest co-fluctuations (Zamani Esfahlani et al. 2020) and that identifiability of individuals was improved by focusing on subsets of time points of intermediate co-fluctuation magnitude (Cutts et al. 2022). We have previously shown a relationship between a time-varying measure of RSNs connectivity and cognitive function (using a sliding window approach) in a cross-sectional sample spanning the AD diagnostic continuum (Chumin et al. 2021). Here, we hypothesized that the application of ETS to group temporally dispersed time points into FC components (FCc), thus separating time points based on co-fluctuation magnitude, would reveal relationships between connectivity and neuropsychological measures that are not detectable and perhaps obscured in conventional 'full FC'.

Methods

Indiana Alzheimer's Disease Research Center (IADRC) Sample. Data were collected at the IADRC, as part of the Indiana Memory and Aging Study, at the Indiana University School of Medicine. Valid datasets (as determined by quality control of image preprocessing) for 152 individuals were included in the present study (Table 1). The sample consisted of 53 cognitively normal controls (CON; no cognitive concerns), 47 subjective cognitive decline participants (SCD; significant cognitive concerns despite normative test performance), 32 mild cognitive impairment participants (MCI; cognitive performance below the normal range), and 20 Alzheimer's disease patients (ALZ). Demographics and neuropsychological domain group comparisons were carried out with a one-way analysis of variance with Tukey-Kramer post hoc tests or chi-squared tests, as appropriate. Informed consent was obtained from all participants or their representatives, and all procedures were approved by the Indiana University Institutional Review board in accordance with the Belmont report. Subsets of the sample have been described in previous publications (Chumin et al. 2021; Contreras et al. 2019).

	Control (CON)	Subjective Cognitive Decline (SCD)	Mild Cognitive Impairment (MCI)	Alzheimer's Disease (ALZ)
N	53	47	32	20
Age (mean ± std. years)	68.2 ± 9.1	69.2 ± 10.8	72.3 ± 7.4	65.9 ± 10.6
Education (mean ± std. years)	16.4 ± 2.3	16.5 ± 2.6	15.8 ± 2.7	15.2 ± 2.5
Sex (Male/Female)	8/45	19/28	17/15	7/13
Race (Caucasian/African American/American Indian)	43/10/0	35/11/1	28/4/0	14/5/1
Cognitive Complaint Index (mean ± std.)	36.8 ± 15	40.2 ± 15.1	38.3 ± 17.8	40.1 ± 15.4
	Domain Scores (z-scored mean ± std.)			
Cognitive	0.47 ± 1.06	-0.02 ± 1.06	-1.75 ± -1.18	-6.23 ± 3.45
Memory	0.00 ± 0.77	-0.13 ± 0.70	-2.04 ± 0.91	-2.99 ± 1.09
Executive	0.12 ± 0.63	0.04 ± 0.60	-0.74 ± 0.78	-1.97 ± 0.99
Language	0.07 ± 0.66	-0.06 ± 0.76	-0.85 ± 0.80	-2.17 ± 1.60
Attention and Processing Speed	0.17 ± 0.80	0.10 ± 0.61	-0.62 ± 0.87	-1.87 ± 1.10
Visuospatial	0.31 ± 1.01	-0.07 ± 1.11	-0.54 ± 1.60	-2.48 ± 4.74

Table 1. Demographic and Neuropsychological Characteristics. Data are shown as counts or mean and standard deviation (std.). Age, years of education, and race distribution did not significantly differ among groups. There was a significant difference in distributions of sex ($X^2(3, N=152) = 14.6$, $p < 0.01$). All six domains showed a significant effect of group (ANOVA, $p < 0.0001$). The four numbers in the right column next to domain names correspond to number of missing data points for each group. Domain scores were derived from the following: Cognitive – Montreal Cognitive Assessment (total score); Memory – Logical Memory (immediate and delayed), CERAD Word List Learning (immediate and delayed), Selective Reminding Test (delayed), 7/24 Spatial Recall Test (immediate & delayed), Rey Auditory Verbal Learning Test (RAVLT; immediate and delayed), Craft stories (immediate and delayed), and Benson Complex Figure (delayed recall); Executive – Digit Span (backwards), Trail Making B, Digit Symbol Substitution, Wisconsin Card Sorting Test (categories & perseverations), Controlled Oral Word Association (COWA), Stroop (Word, Color, and Color-Word scores), UDS3 Letter Fluency; Language - Animal Fluency, Vegetable Fluency, Boston Naming Test, IU Token Test, COWA, Multilingual Naming Test, UDS3 Letter Fluency; Attention and Processing Speed - Digit Span (forward & backward), Trail Making A and B, Digit Symbol, Stroop (Word, Color, & Word/Color); Visuospatial - Benson Complex Figure (copy), Judgement of Line Orientation, Block Design.

IADRC Neuropsychological Scores. Participants completed neuropsychological testing as part of the Uniform Dataset 3.0 (Weintraub et al. 2018), as well as site-specific additional tests. Six domain composite scores were calculated from the following: (1) Cognitive – Montreal Cognitive Assessment (total score) (Nasreddine et al. 2005), (2) Memory – Logical Memory (immediate and delayed) (Wechsler 1987), CERAD Word List Learning (immediate and delayed) (Petersen et al. 1992), Selective Reminding Test (delayed), 7/24 Spatial Recall Test (immediate & delayed), Rey Auditory Verbal Learning Test (RAVLT; immediate and delayed) (Schmidt 1996), Craft stories (immediate and delayed) (Craft et al. 1996), and Benson Complex Figure (delayed recall) (Possin et al. 2011), (3) Executive – Digit Span (backwards) (Ivnik et al. 1992), Trail Making B (Steinberg et al. 2005), Digit Symbol Substitution, Wisconsin Card Sorting Test (categories & perseverations), Controlled Oral Word Association (COWA), Stroop (Word, Color, and Color-Word scores), UDS3 Letter Fluency (Weintraub et al. 2018), (4) Language - Animal Fluency, Vegetable Fluency, Boston Naming Test, IU Token Test, COWA, Multilingual Naming Test, UDS3 Letter Fluency, (5) Attention and Processing Speed - Digit Span (forward & backward), Trail Making A and B, Digit Symbol, Stroop (Word, Color, & Word/Color), (6) Visuospatial - Benson Complex Figure (copy), Judgement of Line Orientation, Block Design. To generate the composite scores, all scores were first adjusted for age, sex, and years of education, *z*-scored relative to a sample of independent (non-overlapping) cognitively normal controls, and then the z-scores were averaged within each domain as described previously (Chumin et al. 2021; Contreras et al. 2019).

IADRC Image Acquisition and Processing. Both image acquisition and preprocessing have been described in detail previously (Chumin et al. 2021). Participants were scanned on a Siemens 3T Prisma Scanner (Siemens, Erlangen, Germany) with a 64-channel head coil. A T1-weighted, whole-brain magnetization prepared rapid gradient echo (MPRAGE) volume was acquired with parameters optimized for the Alzheimer's Disease Neuroimaging Initiative (ADNI 1 & 2; http://adni.loni.usc.edu): 220 sagittal slices, GRAPPA acceleration factor of 2, voxel size 1.1×1.1×1.2 mm^3, duration 5:12 minutes. Two spin-echo echo-planar imaging (12 sec each, TR = 1.56 sec, TE = 49.8 ms, flip angle 90°) volumes were acquired with reverse phase encoding directions for distortion correction. Resting-state functional MRI (rs-fMRI) data were acquired with a gradient-echo echo-planar imaging sequence with a multi-band factor of 3, 10:07 min scan time, and TR of 1.2 sec, resulting in 500 time points. Other relevant parameters were TE = 29 ms, flip angle 65°, 2.5×2.5×2.5 mm^3 voxel size, and 54 interleaved axial slices. During the scan, participants were instructed to remain still with eyes closed and to think of "nothing in particular."

Data were processed with a pipeline developed in-house, implemented in Matlab (MathWorks, version 2019a; Natick, MA), utilizing the Oxford Centre for Functional MRI of the Brain (FMRIB) Software Library (FSL version 6.0.1) (Jenkinson et al. 2012), Analysis of Functional NeuroImages (AFNI; afni.nimh.nih.gov), and ANTS (http://stnava.github.io/ANTs/) packages. This pipeline was developed and optimized for the Siemens scanner data acquired at Indiana University School of Medicine following recommendations in Lindquist et al. (2019); Parkes et al. (2018); Satterthwaite et al. (2013).

All processing was carried out in each participant's native space. T1 volumes were denoised (Coupé et al. 2008), bias field corrected (FSL), and skull stripped (ANTS). rs-fMRI data were first distortion corrected (FSL *topup*), motion corrected (*mcflirt*), and normalized to mode 1000. Nuisance regressors were removed from the data with use of ICA-AROMA (Pruim et al. 2015), aCompCor (Muschelli et al. 2014), and global signal regression. Data were then demeaned, detrended, and bandpass filtered (0.009–0.08 Hz). Finally, 30 time points were removed from the beginning and end of the scan to remove edge artifacts introduced by bandpass filtering and ensure equal binning (see below). Relative frame displacement output by *mcflirt* was used as an index of in-scanner motion.

Cortical Parcellation and Time-Series Extraction. A 200-cortical region brain parcellation was spatially aligned with each subjects' rs-fMRI via the following: (1) linear (6 and 12 degrees of freedom; FSL *flirt*) and nonlinear (FSL *fnirt*) registration of T1 volume, with inverse transformation applied to the Schaefer et al. (2018) 200 node (cortical region) parcellation, (2) dilation and application of a gray matter mask, and (3) registration of T1 to the mean rs-fMRI volume with a linear white matter boundary-based registration (FSL *flirt bbr* cost function). Nodal time-series were then extracted as the mean time course across voxels in each region.

Edge Time-Series and FC Components. ETS were computed as the frame-by-frame product of the z-scored BOLD time-series for all region pairs (19,900 unique edges) (Faskowitz et al. 2020; Jo et al. 2021), resulting in an edge by time matrix of moment-to-moment co-fluctuations (Figure 1A-B), which is analogous to temporally unwrapping the Pearson correlation (the mean over time of ETS is equal to the conventional "full FC" or "static FC"). The ETS matrix was then used to compute root-sum-square (RSS) at each time point as an index of global co-fluctuation amplitude (Figure 1C). RSS ranked time points were then divided into 5 equally sized bins (43 TRs per bin, ~52 second of noncontiguous data). The mean edgewise co-fluctuation within each bin was then computed and is referred to as an FC component (Figure 1D). Each component is thought of as a representation of co-fluctuation within its RSS band, and we hypothesized that different FC components would differentially associate with neurocognitive domains.

Network Contingency Correlation (NCC) Analysis Framework. To identify relationships between neuropsychological domains and FC (full and RSS components), a modified network contingency analysis (NCA) (Contreras et al. 2019; Sripada et al. 2014) was employed. The NCA framework uses a *t*-test to compute edge-level group differences, then counts the number of significant edges within blocks (i.e., RSNs) and determines block-level significance relative to a permuted data null. This method sidesteps the limitation of mass univariate testing, without averaging data and diluting potential effects. Here, in formulating NCC, the group inference via *t*-test was replaced by a Spearman correlation, quantifying the relationship between individual network edges and behavioral measures. The NCC procedure is applied as follows: (1) edgewise correlations are computed between FC (full or component) and a behavioral domain score, which yields a matrix of correlation coefficients and a binary significance matrix (here the edge-level threshold was set at $p < 0.01$; Figure 1E-F), (2) data are permuted (we tested two null models: a block permutation where RSNs assignment are scrambled and a score permutation where the behavioral scores are scrambled across subjects; Figure 1G) and a distribution of null significance matrices is generated (5,000 permutations, Figure 1H)), (3) the block structure is imposed on the empirical and null significance networks (here we used the 7 canonical RSNs described Yeo et al. (2011) (visual, somatomotor, dorsal and ventral attention, limbic, frontoparietal, and default mode) with node assignments provided in Schaefer et al. (2018)) and the number of significant edges is counted for all within- and between-RSN blocks, and (4) block-level significance *p*-value is defined as one minus the fraction of instances where the count of significant edges in a block exceeded the null, followed by a false discovery rate (FDR) adjustment for number of blocks (7 within and 21 between RSN) at $q < 0.05$ (Figure 1I). An exploratory run of NCC was also performed without imposing a block structure (i.e., treating all nodes as belonging to one block) and using a network-based statistics largest connected component-based correction with an initial edge-level threshold of $p < 0.01$ (Zalesky et al. 2010).

Results

Demographic group comparisons. No differences in age (ANOVA, $F(3,148)=2.07$, $p > 0.05$), education ($F(3,148)=1.54$, $p > 0.05$), or race ($X^2(3, N=152) = 5.5$, $p > 0.05$) were observed. There were proportionally more female participants in the CON and SCD groups ($X^2(3, N=152) = 14.6$, $p < 0.01$). All neuropsychological domains showed a significant main effect of group (ANOVA: Cognitive $F(3,142) = 87.9$, Memory $F(3,142) = 85.4$, Executive $F(3,140) = 39.6$, Language $F(3,140) = 30.1$, Attention and Processing Speed $F(3,141) = 28.7$, and Visuospatial $F(3,139) = 8.7$, all $p < 0.0001$). Post hoc testing showed that for 4 domains (not including memory and visuospatial) only CON v. SCD comparisons were not significant ($p > 0.05$). For the memory domain CON v. SCD and MCI v. ALZ were not significant ($p > 0.05$). Finally, only the pairwise comparisons against the ALZ group were significant for the visuospatial domain ($p < 0.05$).

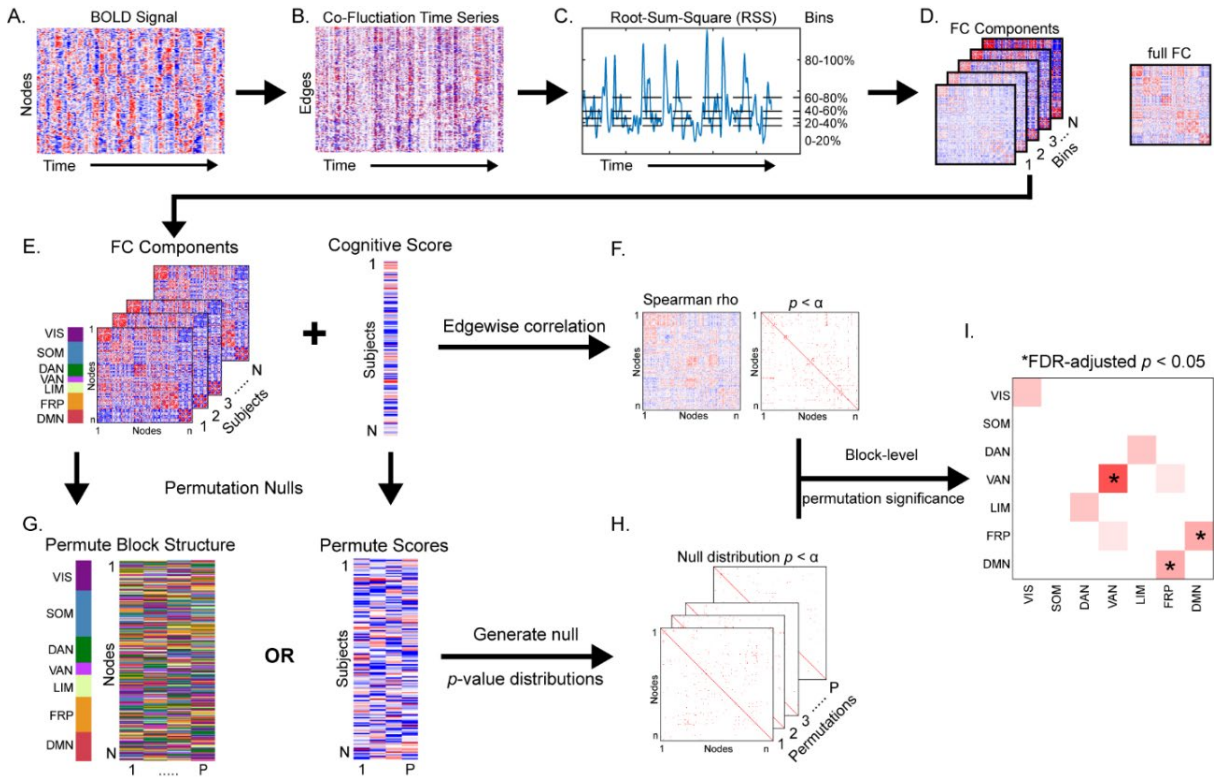

Figure 1. Edge time-series, functional connectivity (FC) components, and Network Contingency Correlation. (A) Blood-oxygen-level-dependent (BOLD) time-series are z-scored and multiplied for all node pairs to yield (B) edge time-series that describe moment-to-moment co-fluctuation among regions. (C) Root-sum-square (RSS), an index of total co-fluctuation magnitude, is computed at each time point and used to rank and parse time points into equally sized bins, with the mean within each bin corresponding to (D) an FC component. Additionally, full FC is computed as the mean of all time points and is equivalent to Pearson correlation. (E) FCC estimates are correlated at each edge with cognitive domain scores of interest to generate (F) a correlation and a *p*-value matrix. (G) A permutation null (either scrambling the network block structure or cognitive domain scores) is then employed to generate (H) a set of null matrices. (I) Network-block level significance is then computed as a permutation *p*-value (one minus the number of times the count of significant edges within a block in empirical data exceeded null data). *p*-value is then adjusted for number of blocks tested with false discovery rate (FDR) correction. VIS – visual, SOM – somatomotor, DAN – dorsal attention, VAN – ventral attention, LIM – limbic, FRP – frontoparietal, DMN – default mode network.

Characterization of RSS quantile FCc. Group-averaged FC and FCc matrices are shown in Figure 2. FC (correlation matrices; Figure 2A) are bounded [-1 1], while FCc matrices of average co-fluctuation within RSS quantiles are not, as evident by increasing amplitude with increasing RSS quantile. To determine if there is unique information within each FCc, we cross-correlated all participants to assess their similarity (Figure 3A). Full FC showed highest correlation values approaching Pearson r values of +0.6. Subject cross-correlation qualitatively increased for increasing RSS quantile FCc; however, they stayed below full FC, suggesting greater relative inter-subject variability. No relationship to in-scanner motion (frame displacement) was found for single time point RSS values in this sample (Pearson r = 0.05, Figure 3B). Comparisons of group average FCc (visualized in Figure 2B-F) showed that ALZ group FCcs were least correlated with the other 3 diagnostic groups and that within group, FCcs from distant RSS quantiles had lower correlation values (Figure 3C). Finally, as shown in previous work where top 5% RSS time points were highly correlated with FC (Zamani Esfahlani et al. 2020), when correlating quantile FCcs to full FC, components derived from greater RSS percentiles (higher co-fluctuation time points) were more similar to full FC (Figure 3D).

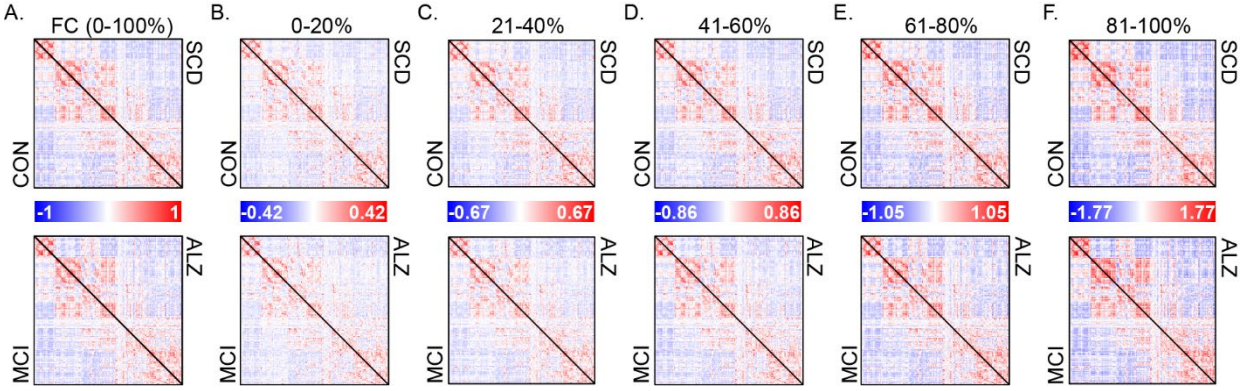

Figure 2. Group averaged full functional connectivity (FC) and its components. (A) Average group full functional connectivity computed as Pearson correlation, which is equivalent to the average co-fluctuation of all time points. Each triangle within a matrix is a group averaged network of unique edges: Controls (CON) – top matrix lower triangle, subjective cognitive decline (SCD) – top matrix upper triangle, mild cognitive impairment (MCI) – bottom matrix lower triangle, and Alzheimer's disease (ALZ) – bottom matrix upper triangle. (B-F) Group averaged FC components, each comprised of 20% of root sum square (RSS) ranked time points, with 0-20% corresponding to lowest RSS amplitude bin, and 80-100% to the highest amplitude.

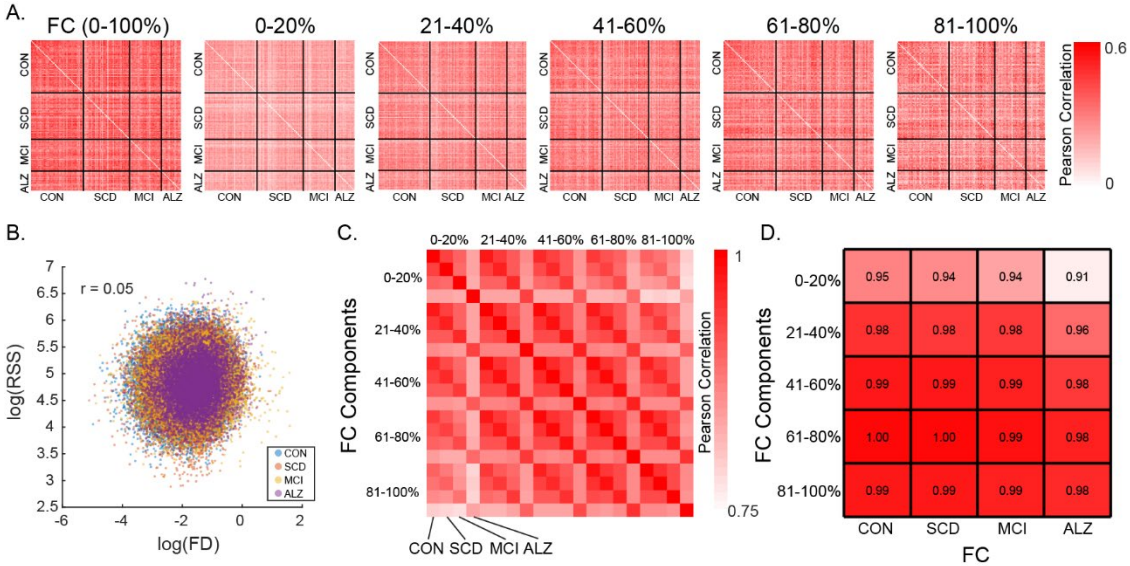

Figure 3. Similarity among FC and its components and relationship of root-sum-square (RSS) with in-scanner motion. (A) Cross-correlation among participants (ordered by diagnostic group) of full FC and the 5 RSS FC components. (B) Scatter correlation (Pearson r) of RSS and frame displacement (FD) shown in log scale and colored by diagnostic group. (C) Cross-correlation (Pearson r) of group averaged FC components ordered by increasing RSS bin and by group within each bin. (D) Correlation of group averaged full FC to each of the RSS FC components split by group. CON – Controls, SCD – subjective cognitive decline, MCI – mild cognitive impairment, ALZ – Alzheimer's disease.

Network Contingency Correlation. Analysis of FC/FCc relationships with neuropsychological domain scores showed that permutation of domain scores was a more conservative strategy compared to RSN block label permutation (Supplementary Figures 1, 2). While the purpose of the score permutation null is to destroy the subject connectivity-behavior relationship to test if number of significant edges in a block is meaningful, the purpose of the block structure permutation null is to assess if the distribution of significant edges is clustered within a particular block. Therefore, by focusing only on RSN blocks that were identified in both strategies, we determine whether the number and the

distribution of significance in a block is robust. The cognitive domain was the only one to show significant relationships for both FC and FCc bins for the ventral attention network (RSS quantiles 40-60% and 60-80%, Figure 4A, D-E). Association between the visual system and the cognitive domain was also observed, but only for FC (Figure 4A). The remaining associations with the cognitive domain were identified in between system interaction blocks: limbic-dorsal attention (0-20% and 80-100% RSS FCc, Figure 4B, F), frontoparietal-default mode interaction (20-40% FCc, Figure 4C), and the frontoparietal-visual interaction blocks (60-80% FCc, Figure 4E). In addition, the executive function domain associated with the limbic-dorsal attention interaction block (0-20% FCc, Figure 4G), the language domain associated with the dorsal attention block (40-60% and 60-80% FCc, Figure 4H-I), and the attention and processing speed domain associated with the frontoparietal system (20-40% FCc, Figure 4J). Across both null strategies and all comparisons, the upper bound of the percent of significant edges (normalized by the size of the RSN block) was 8%. While this is a relatively small fraction of total edges within a network block, each edge passed the initial $p < 0.01$ significance threshold, with the blocks achieving FDR-adjusted significance of $p < 0.05$ (corrected for 7 within and 21 between RSN blocks tested for each domain). To assess the impact of number of bins, the analysis was repeated with 10 FCcs and similar results were obtained (Supplementary Figure 3), which largely identified the same RSS percentile components and neuropsychological domains.

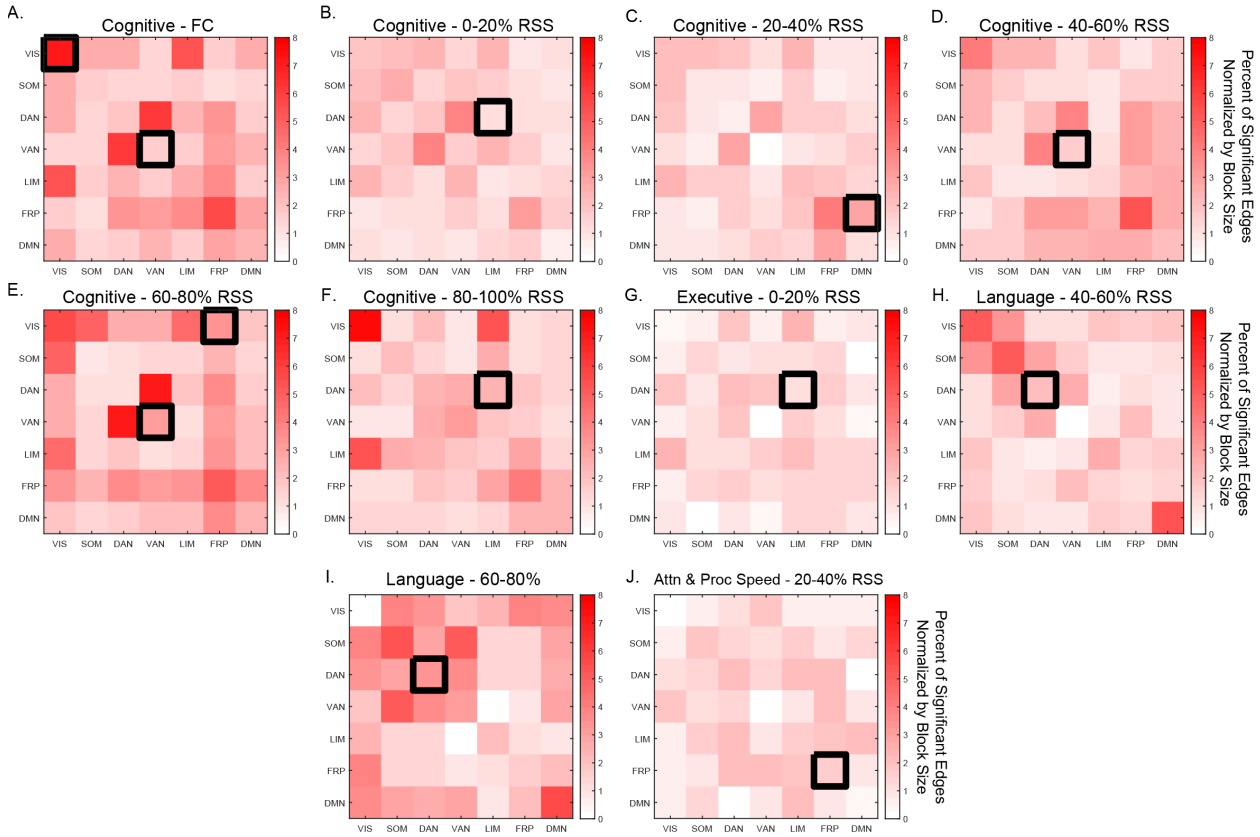

Figure 4. Network Contingency Correlation (NCC) resting state network block-level results. Matrices show percent of edges by block (normalized by size of block) that passed initial uncorrected edge-level significance of $p < 0.001$. Black boxes denote block-level significance of $p_{FDR} < 0.05$, with 5,000 NCC permutations. Only blocks that were significant against both permutation nulls are shown. Upper and lower triangular of matrices are identical; significance is only shown on the upper triangle. FC – functional connectivity, RSS – root sum squared. Attn & Proc Speed – attention and processing speed. Resting state networks: VIS – visual, SOM – somatomotor, DAN – dorsal attention, VAN – ventral attention, LIM – limbic, FRP – frontoparietal, DMN – default mode network.

Exploratory Network-Based Statistics (NBS) Component Analysis. NBS employs permutation testing to identify connected clusters of nodes above a random null. Six clusters were identified: three associated with the cognitive domain, including

full FC (Figure 5A), 40-60% RSS range-derived FCc (Figure 5B), and 60-80% FCc (Figure 5C), one association between the executive domain and 60-80% FCc (Figure 5D), and two associations between the language domain and 40-60% FCc, as well as 60-80% FCc, edges (Figure 5E-F). Degree distributions show that these are extensively interconnected components with multiple neighbors to most nodes, while the matrices show that they are composed of both positive and negative correlations with behavior. These components differ in their composition depending on FC component and domains being compared and are largely characterized by positive within-RSN and negative between-RSN edges (although this is not ubiquitous; see Figure 5C and 5D for notable examples of positive associations between RSN connectivity and cognitive and executive domains, respectively).

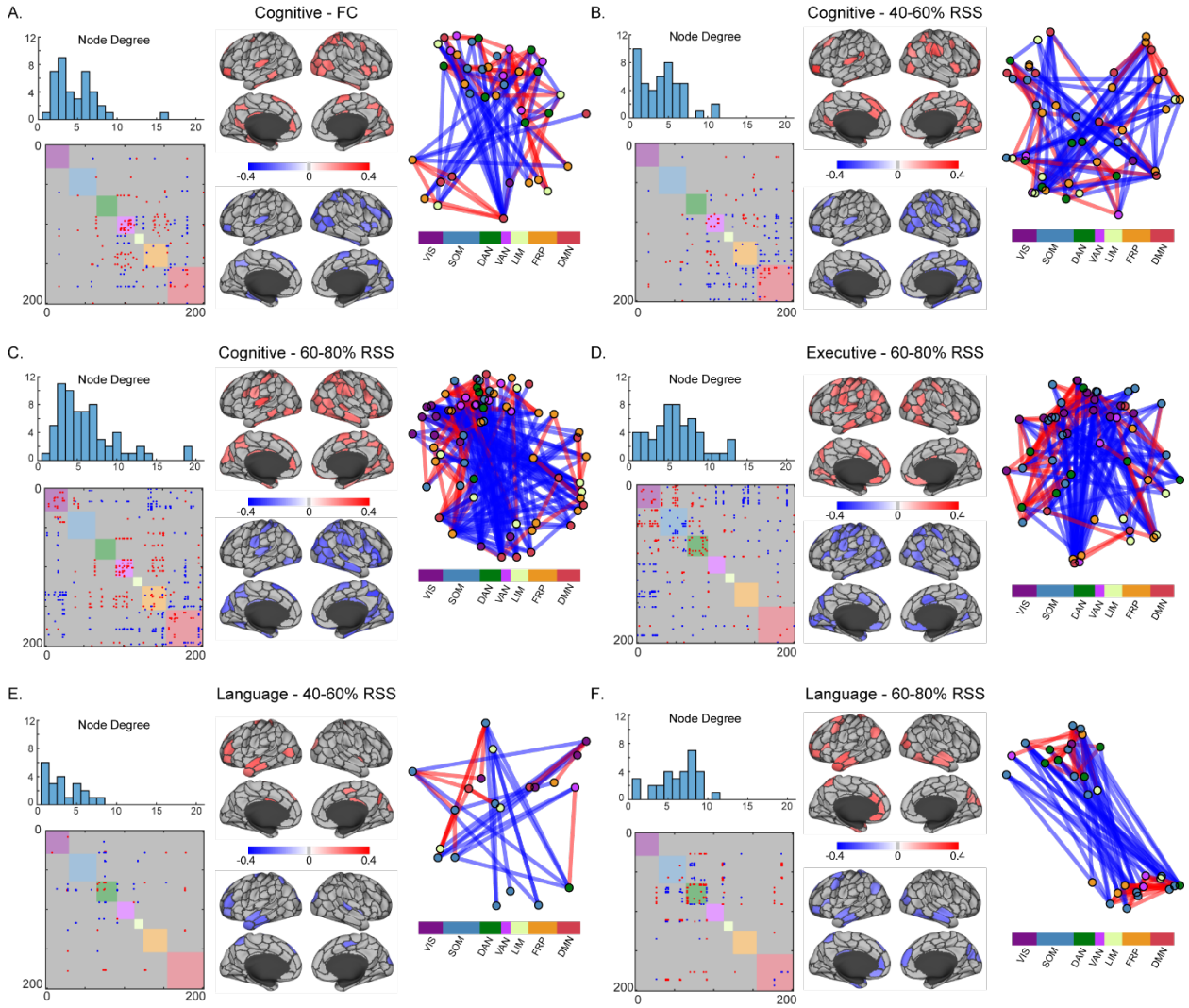

Figure 5. Block-free Network-Based Statistics significant FC component-neuropsychological domain correlations. For each of the six significant components identified across six neuropsychological domains and five FC components and full FC, (upper-left) histograms show nodal degree distributions, (lower-left) matrices show binary positively and negatively correlated edges within each component, (middle) Schaefer 200-node cortical parcellations show average positive and negative edge correlations for component nodes, (right) a force-directed diagram from component nodes colored by Yeo systems and edges colored as positively (red) or negatively (blue) correlated with the neuropsychological domain of interest, shown using an inverse weighting visualization, such that higher edge weights yield shorter distances. System labels are VIS-Visual, SOM-Somatomotor, DAN-Dorsal Attention, VAN-Ventral Attention, LIM-Limbic, FRP-Frontoparietal, DMN-Default Mode. Root-sum-square (RSS) percentiles refer to boundaries of RSS values from which FC components were computed.

Discussion

The identification of robust and reproducible brain-behavior relationships has significant implications for neuroscience. Their reliable detection in noninvasive fMRI data presents a tremendous challenge, as their expression may be highly time and context dependent. Here, in the context of AD, we presented findings from application of a single time point fMRI framework (edge time-series), in order to assess whether certain moments in time (as indexed by root sum squared (RSS) ranked co-fluctuations), are preferentially correlated with neuropsychological performance in a cross-sectional sample that spans the AD diagnostic spectrum. Employing block-level inference we identified RSNs and RSN interactions of FC components (FCcs) that correlated with neuropsychological function domains. Aside from full FC of the ventral attention network and its correlation with the cognitive function domain, the identified relationships were not significant when using conventional/static FC (cross-correlation of the full time-series). The appearance of the association between cognitive function and FC of the ventral attention system confirms previous findings obtained with sliding-window dynamic FC that its temporal properties are robustly related to cognitive function (Chumin et al. 2021).

Single-TR decomposition of fMRI edge time series allows for many possible strategies to generate FCcs. Here we divided the fMRI time series into 5 equal bins based on ranking time points by their overall co-fluctuation amplitude (RSS), yielding 5 FCcs. We found that the cognitive domain showed the highest number of associations with FCc RSN blocks across all 5 RSS bins, with notable RSN blocks including the attentional systems (ventral and dorsal attention-limbic interaction). This is consistent with functional interactions of attentional systems and cognitive function, resource recruitment, and reserve (Anthony and Lin 2018; Bastin et al. 2012; Gordon et al. 2015; Zhang et al. 2015). Blocks that included the dorsal attention system were also identified to relate to executive and language domains. Additionally, the frontoparietal control system and its interactions with other RSNs appears for cognitive and attention domains at two RSS bins. These relationships are not found in the full FC matrix, 'obscured' by the high co-fluctuation time points that drive the RSN block structure observed in human rs-fMRI.

There is a distinction between the broadly applied sliding window methods in AD and the ETS approach (Faskowitz et al. 2022; Lurie et al. 2020). Both operate on subsets of data; however, ETS rely on a single time point decomposition of the Pearson correlation, making no assumptions about the duration of underlying dynamics. Operating on a shorter time scale with ETS is beneficial, as it better characterizes the ongoing dynamics and has a narrow autocorrelation structure. A second distinction between ETS and previous methodology is that here connectivity of specific systems is being investigated. To date, studies that have employed sliding window FC to study AD have relied on clustering of group connectivity patterns into states. This is a data reduction strategy, as properties of connectivity states (i.e., frequency and dwell time) are then used as predictors/outcomes for statistical analysis. While this is a reasonable approach, it tests whether a property of a state, which is a whole-brain descriptor, is related to behavior of interest. Systems within the brain are likely to differentially relate to behavior, so properties of states, which are whole network descriptors, are unlikely to robustly relate to behaviors. Therefore, a focus on subsystems within the brain, which share some intrinsic properties, may allow us to identify robust behavioral correlates.

The strategy undertaken here (system/block level inference) is also one of data reduction, aimed at avoiding mass univariate tests in order to obtain interpretable outcomes. However, unlike sliding window, data reduction is caried out during inference through application of frequency statistics. The network contingency analysis proposed by Sripada et al. (2014) was developed to identify block-level group differences between networks, by testing whether the number of significantly different edges in a block exceeded the number expected to occur by chance (with permutation testing). Here we modified this framework for use with correlations, proposing two permutation null strategies for assessment of block-level brain-behavior relationships. The two strategies each permute one of two variables of interest (either FC or behavior), testing whether the observed edge relationships preferentially cluster within a block or if the number of edge-level correlation exceeds the null distribution, respectively. The joined significance against the two models then describes whether the relationships within an RSN block are significant both in number and spatial distribution within the network.

A similar approach to linking fMRI to behavioral and/or neuropsychological measures as the one employed here is connectome-based predictive modeling (CPM), which relies on a cross-validation strategy to build behavior predictive models, by first selecting a subset of edges with the strongest relationship to the behavior of interest (Finn et al. 2015; Shen et al. 2017). These edges can then be qualitatively described in terms of which regions/systems they are comprised of. This strategy has been applied in AD (Lin et al. 2018; Svaldi et al. 2021). Svaldi et al. (2021) employed a dual approach whereby FC data were first subjected to a principal component analysis (PCA)-based procedure aimed at improving participant identifiability. They then showed that the new FC matrices resulted in improved CPM performance to predict AD-relevant cognitive measures. Interestingly, Mantwill et al. (2022) recently showed that (at least in the young and healthy Human Connectome Project cohort) identifiability and behavior prediction are reliant upon distinct functional systems. Given this evidence it is unclear how a PCA-based improvement of FC aimed at identifiability impacts behavioral prediction. Analogous to Svaldi et al. (2021), which posited that FC matrices from PCA component sets have more relevance to behavior than full FC, we hypothesized that particular time points may be more relevant, thereby parsing them into bins based on co-fluctuation magnitude to estimate FC components.

We conducted an exploratory analysis where a RSN block structure was not imposed on FC components. Treating the whole network as a single block, we looked for connected components that significantly correlated with neuropsychological domains using the network-based statistics correction strategy (Zalesky et al. 2010). As with the NCC strategy only, the cognitive function domain was correlated with FC, composed of a component that included the ventral attention network and its interactions with frontoparietal and default mode networks. Upper middle RSS bin components revealed significant components that seem to differ in their spatial distribution for each neuropsychological domain (Figure 5 shows primarily (1) ventral attention, frontoparietal and default mode relationships with cognitive, (2) visual, somatomotor, and dorsal attention interactions with other systems for executive, and (3) dorsal attention for language neuropsychological domains).

It is important to consider these findings within the constraints of the methodology and analyses employed. First, this is a cross-sectional investigation with the sample spanning the AD diagnostic continuum, aimed at investigating how FC components are altered in relation to disease-relevant neuropsychological domains. Future longitudinal follow-ups are necessary to assess whether this strategy reveals similar relationships in within-subject designs. Second, we chose a 200-region functional cortical parcellation (Schaefer et al. 2018) stratified into seven canonical RSNs (Yeo et al. 2011). Whether the same or similar systems are implicated utilizing different parcellation and network stratifications can be a topic of future investigations, as node selection is often debated in network neuroscience and can be a source of variance in network data (Domhof et al. 2021). Additional inclusion of subcortical, cerebellar, and brainstem regions may shed light on relationships between neuropsychological function and interactions between cortical systems and the subcortex. Finally, because of the frequency statistic-based testing of block-level relationships employed by NCC, we cannot, or rather should not, conduct follow-up tests to isolate the significant edges within blocks. Therefore, this method is limited in its interpretation as to whether or not there is a coupling between FC and behavior for a set of subsystems (here RSNs) only.

In summary, we hypothesized that a decomposition of FC into components derived from temporally discrete data points via an edge time series summary metric that indexes magnitude of co-fluctuation in a network will reveal brain-behavior relationships not observed with conventional full FC. Applied to a sample that spans the AD diagnostic spectrum, we show that discrete FC components are related to neuropsychological domain performance within and between specific RSN systems. This work can serve as a starting point for more targeted investigations of specific brain systems and how they relate to phenotypic changes as a consequence of AD and related dementias.

Declarations

Ethical Approval. Informed consent was obtained from all participants or their representatives, and all procedures were approved by the Indiana University Institutional Review board in accordance with the Belmont report.

Competing Interests. The authors have no competing interests, or other interests that might be perceived to influence the results and/or discussion reported in this paper.

Author Contributions. Evgeny J. Chumin: Conceptualization, Methodology, Formal analysis, Software, Writing - original draft, Writing - review & editing. **Sarah A. Cutts**: Conceptualization, Methodology, Writing - review & editing. **Shannon L. Risacher**: Methodology, Resources, Data curation, Funding acquisition, Writing - review & editing. **Liana G. Apostolova**: Methodology, Funding acquisition, Writing - review & editing. **Martin R. Farlow**: Writing - review & editing. **Brenna C. McDonald**: Writing - review & editing. **Yu-Chien Wu**: Writing - review & editing, Funding acquisition. **Richard Betzel**: Conceptualization, Methodology, Writing - review & editing. **Andrew J. Saykin**: Supervision, Funding acquisition, Writing - review & editing. **Olaf Sporns**: Conceptualization, Methodology, Software, Supervision, Writing - review & editing.

Funding. This work was supported by the National Institute on Aging (R01 AG019771, P30 AG10133, K01 AG049050, R01 AG061788), the National Institute for Complementary and Integrative Health (R01 AT009036-03), the Indiana University Network Science Institute, the Department of Radiology and Imaging Sciences, the Indiana University Health-Indiana University School of Medicine Strategic Research Initiative, and the Indiana Clinical and Translational Sciences Institute (CTSI). Part of this research was also supported in part by Lilly Endowment, Inc., through its support for the Indiana University Pervasive Technology Institute, and in part by the Indiana METACyt Initiative. The Indiana METACyt Initiative at Indiana University was also supported in part by Lilly Endowment, Inc. This material is based upon work supported by the National Science Foundation under grant no. CNS-0521433.

Data Availability. Data access can be obtained by contacting the Indiana Alzheimer's Disease Center Data Core.

Acknowledgements. The authors thank Eileen Tallman, Aaron Vosmeier, Rachael Deardorff, Bradley Glazier, Kala Hall, Lili Kyurkchiyska, Evan Finley, Yolanda Graham-Dotson, Steve Brown, and Sujuan Gao for their contributions to this study. We also thank the participants in the Indiana Memory and Aging Study (IMAS) and their family members, without whom this research would not be possible. The authors also acknowledge the Indiana University Pervasive Technology Institute (Stewart et al. 2017) for providing supercomputing and storage resources, supported in part by Lilly Endowment, Inc., through its support for the Indiana University Pervasive Technology Institute.

References

Anthony M, Lin F (2018) A Systematic Review for Functional Neuroimaging Studies of Cognitive Reserve Across the Cognitive Aging Spectrum. Archives of Clinical Neuropsychology 33: 937-948.

Bastin C, Yakushev I, Bahri MA, Fellgiebel A, Eustache F, Landeau B, Scheurich A, Feyers D, Collette F, Chételat G, Salmon E (2012) Cognitive reserve impacts on inter-individual variability in resting-state cerebral metabolism in normal aging. NeuroImage 63: 713-722.

Betzel RF, Cutts SA, Greenwell S, Faskowitz J, Sporns O (2022) Individualized event structure drives individual differences in whole-brain functional connectivity. NeuroImage 252: 118993.

Buckner RL, Andrews-Hanna JR, Schacter DL (2008) The Brain's Default Network. Annals of the New York Academy of Sciences 1124: 1-38.

Calhoun Vince D, Miller R, Pearlson G, Adalı T (2014) The Chronnectome: Time-Varying Connectivity Networks as the Next Frontier in fMRI Data Discovery. Neuron 84: 262-274.

Chumin EJ, Risacher SL, West JD, Apostolova LG, Farlow MR, McDonald BC, Wu YC, Saykin AJ, Sporns O (2021) Temporal stability of the ventral attention network and general cognition along the Alzheimer's disease spectrum. NeuroImage Clinical 31: 102726.

Cohen JR (2018) The behavioral and cognitive relevance of time-varying, dynamic changes in functional connectivity. NeuroImage 180: 515-525.

Contreras JA, Avena-Koenigsberger A, Risacher SL, West JD, Tallman E, McDonald BC, Farlow MR, Apostolova LG, Goñi J, Dzemidzic M, Wu Y-C, Kessler D, Jeub L, Fortunato S, Saykin AJ, Sporns O (2019) Resting state network modularity along the prodromal late onset Alzheimer's disease continuum. NeuroImage: Clinical 22: 101687.

Coupé P, Yger P, Prima S, Hellier P, Kervrann C, Barillot C (2008) An Optimized Blockwise Nonlocal Means Denoising Filter for 3-D Magnetic Resonance Images. Medical Imaging, IEEE Transactions on 27: 425-441.

Craft S, Newcomer J, Kanne S, Dagogo-Jack S, Cryer P, Sheline Y, Luby J, Dagogo-Jack A, Alderson A (1996) Memory improvement following induced hyperinsulinemia in alzheimer's disease. Neurobiology of Aging 17: 123-130.

Cutts SA, Faskowitz J, Betzel RF, Sporns O (2022) Uncovering individual differences in fine-scale dynamics of functional connectivity. Cerebral cortex: bhac214.

Dai Z, Lin Q, Li T, Wang X, Yuan H, Yu X, He Y, Wang H (2019) Disrupted structural and functional brain networks in Alzheimer's disease. Neurobiology of Aging 75: 71-82.

Dai Z, Yan C, Li K, Wang Z, Wang J, Cao M, Lin Q, Shu N, Xia M, Bi Y, He Y (2015) Identifying and Mapping Connectivity Patterns of Brain Network Hubs in Alzheimer's Disease. Cerebral cortex 25: 3723-3742.

Domhof JWM, Jung K, Eickhoff SB, Popovych OV (2021) Parcellation-induced variation of empirical and simulated brain connectomes at group and subject levels. Network Neuroscience 5: 798-830.

Faskowitz J, Betzel RF, Sporns O (2022) Edges in brain networks: Contributions to models of structure and function. Network Neuroscience 6: 1-28.

Faskowitz J, Esfahlani FZ, Jo Y, Sporns O, Betzel RF (2020) Edge-centric functional network representations of human cerebral cortex reveal overlapping system-level architecture. Nature neuroscience 23: 1644-1654.

Finn ES, Shen X, Scheinost D, Rosenberg MD, Huang J, Chun MM, Papademetris X, Constable RT (2015) Functional connectome fingerprinting: identifying individuals using patterns of brain connectivity. Nature neuroscience 18: 1664-1671.

Forouzannezhad P, Abbaspour A, Fang C, Cabrerizo M, Loewenstein D, Duara R, Adjouadi M (2019) A survey on applications and analysis methods of functional magnetic resonance imaging for Alzheimer’s disease. Journal of Neuroscience Methods 317: 121-140.

Fox MD, Corbetta M, Snyder AZ, Vincent JL, Raichle ME (2006) Spontaneous neuronal activity distinguishes human dorsal and ventral attention systems. Proceedings of the National Academy of Sciences 103: 10046-10051.

Franzmeier N, Buerger K, Teipel S, Stern Y, Dichgans M, Ewers M (2017) Cognitive reserve moderates the association between functional network anti-correlations and memory in MCI. Neurobiology of Aging 50: 152-162.

Franzmeier N, Neitzel J, Rubinski A, Smith R, Strandberg O, Ossenkoppele R, Hansson O, Ewers M (2020) Functional brain architecture is associated with the rate of tau accumulation in Alzheimer’s disease. Nature Communications 11: 347.

Franzmeier N, Rubinski A, Neitzel J, Kim Y, Damm A, Na DL, Kim HJ, Lyoo CH, Cho H, Finsterwalder S, Duering M, Seo SW, Ewers M (2019) Functional connectivity associated with tau levels in ageing, Alzheimer’s, and small vessel disease. Brain 142: 1093-1107.

Gordon BA, Zacks JM, Blazey T, Benzinger TLS, Morris JC, Fagan AM, Holtzman DM, Balota DA (2015) Task-evoked fMRI changes in attention networks are associated with preclinical Alzheimer’s disease biomarkers. Neurobiology of Aging 36: 1771-1779.

Hutchison RM, Womelsdorf T, Allen EA, Bandettini PA, Calhoun VD, Corbetta M, Della Penna S, Duyn JH, Glover GH, Gonzalez-Castillo J, Handwerker DA, Keilholz S, Kiviniemi V, Leopold DA, de Pasquale F, Sporns O, Walter M, Chang C (2013) Dynamic functional connectivity: Promise, issues, and interpretations. NeuroImage 80: 360-378.

Idesis S, Faskowitz J, Betzel RF, Corbetta M, Sporns O, Deco G (2022) Edge-centric analysis of stroke patients: An alternative approach for biomarkers of lesion recovery. NeuroImage: Clinical 35: 103055.

Ivnik RJ, Malec JF, Smith GE, Tangalos EG, Petersen RC, Kokmen E, Kurland LT (1992) Mayo's older americans normative studies: WAIS-R norms for ages 56 to 97. Clinical Neuropsychologist 6: 1-30.

Jenkinson M, Beckmann CF, Behrens TEJ, Woolrich MW, Smith SM (2012) FSL. NeuroImage 62: 782-790.

Jo Y, Zamani Esfahlani F, Faskowitz J, Chumin EJ, Sporns O, Betzel RF (2021) The diversity and multiplexity of edge communities within and between brain systems. Cell Rep 37: 110032.

Lin Q, Rosenberg MD, Yoo K, Hsu TW, O'Connell TP, Chun MM (2018) Resting-State Functional Connectivity Predicts Cognitive Impairment Related to Alzheimer's Disease. Frontiers in Aging Neuroscience 10.

Lindquist MA, Geuter S, Wager TD, Caffo BS (2019) Modular preprocessing pipelines can reintroduce artifacts into fMRI data. Human Brain Mapping 40: 2358-2376.

Lurie DJ, Kessler D, Bassett DS, Betzel RF, Breakspear M, Kheilholz S, Kucyi A, Liégeois R, Lindquist MA, McIntosh AR, Poldrack RA, Shine JM, Thompson WH, Bielczyk NZ, Douw L, Kraft D, Miller RL, Muthuraman M, Pasquini L, Razi A, Vidaurre D, Xie H, Calhoun VD (2020) Questions and controversies in the study of time-varying functional connectivity in resting fMRI. Network Neuroscience 4: 30-69.

Mantwill M, Gell M, Krohn S, Finke C (2022) Brain connectivity fingerprinting and behavioural prediction rest on distinct functional systems of the human connectome. Communications Biology 5: 261.

Muschelli J, Nebel MB, Caffo BS, Barber AD, Pekar JJ, Mostofsky SH (2014) Reduction of motion-related artifacts in resting state fMRI using aCompCor. NeuroImage 96: 22-35.

Nasreddine ZS, Phillips NA, Bédirian V, Charbonneau S, Whitehead V, Collin I, Cummings JL, Chertkow H (2005) The Montreal Cognitive Assessment, MoCA: A Brief Screening Tool For Mild Cognitive Impairment. Journal of the American Geriatrics Society 53: 695-699.

Parkes L, Fulcher B, Yücel M, Fornito A (2018) An evaluation of the efficacy, reliability, and sensitivity of motion correction strategies for resting-state functional MRI. NeuroImage 171: 415-436.

Petersen RC, Smith G, Kokmen E, Ivnik RJ, Tangalos EG (1992) Memory function in normal aging. Neurology 42: 396-401.

Possin KL, Laluz VR, Alcantar OZ, Miller BL, Kramer JH (2011) Distinct neuroanatomical substrates and cognitive mechanisms of figure copy performance in Alzheimer's disease and behavioral variant frontotemporal dementia. Neuropsychologia 49: 43-48.

Pruim RHR, Mennes M, van Rooij D, Llera A, Buitelaar JK, Beckmann CF (2015) ICA-AROMA: A robust ICA-based strategy for removing motion artifacts from fMRI data. NeuroImage 112: 267-277.

Sasse L, Larabi DI, Omidvarnia A, Jung K, Hoffstaedter F, Jocham G, Eickhoff SB, Patil KR (2022) Intermediately Synchronised Brain States optimise trade-off between Subject Identifiability and Predictive Capacity. bioRxiv: 2022.09.30.510304.

Satterthwaite TD, Elliott MA, Gerraty RT, Ruparel K, Loughead J, Calkins ME, Eickhoff SB, Hakonarson H, Gur RC, Gur RE, Wolf DH (2013) An improved framework for confound regression and filtering for control of motion artifact in the preprocessing of resting-state functional connectivity data. NeuroImage 64: 240-256.

Schaefer A, Kong R, Gordon EM, Laumann TO, Zuo X-N, Holmes AJ, Eickhoff SB, Yeo BTT (2018) Local-Global Parcellation of the Human Cerebral Cortex from Intrinsic Functional Connectivity MRI. Cerebral cortex 28: 3095-3114.

Schmidt M (1996) Rey Auditory and Verbal Learning Test. A Handbook. Western Psychological Association

Schumacher J, Peraza LR, Firbank M, Thomas AJ, Kaiser M, Gallagher P, O'Brien JT, Blamire AM, Taylor J-P (2019) Dynamic functional connectivity changes in dementia with Lewy bodies and Alzheimer's disease. NeuroImage: Clinical 22: 101812.

Shen X, Finn ES, Scheinost D, Rosenberg MD, Chun MM, Papademetris X, Constable RT (2017) Using connectome-based predictive modeling to predict individual behavior from brain connectivity. Nature protocols 12: 506-518.

Smith RX, Strain JF, Tanenbaum A, Fagan AM, Hassenstab J, McDade E, Schindler SE, Gordon BA, Xiong C, Chhatwal J, Jack C, Karch C, Berman S, Brosch JR, Lah JJ, Brickman AM, Cash DM, Fox NC, Graff-Radford NR, Levin J, Noble J, Holtzman DM, Masters CL, Farlow MR, Laske C, Schofield PR, Marcus DS, Morris JC, Benzinger TLS, Bateman RJ, Ances BM (2021) Resting-State Functional Connectivity Disruption as a Pathological Biomarker in Autosomal Dominant Alzheimer Disease. Brain Connectivity 11: 239-249.

Sripada C, Kessler D, Fang Y, Welsh RC, Prem Kumar K, Angstadt M (2014) Disrupted network architecture of the resting brain in attention-deficit/hyperactivity disorder. Human Brain Mapping 35: 4693-4705.

Steinberg BA, Bieliauskas LA, Smith GE, Ivnik RJ, Malec JF (2005) Mayo's Older Americans Normative Studies: Age- and IQ-Adjusted Norms for the Auditory Verbal Learning Test and the Visual Spatial Learning Test. Clin Neuropsychol 19: 464-523.

Stewart CA, Welch V, Plale B, Fox G, Pierce M, Sterling T (2017) Indiana University Pervasive Technology Institute.

Svaldi DO, Goñi J, Abbas K, Amico E, Clark DG, Muralidharan C, Dzemidzic M, West JD, Risacher SL, Saykin AJ, Apostolova LG (2021) Optimizing differential identifiability improves connectome predictive modeling of cognitive deficits from functional connectivity in Alzheimer's disease. Human Brain Mapping 42: 3500-3516.

Therriault J, Zimmer ER, Benedet AL, Pascoal TA, Gauthier S, Rosa-Neto P (2022) Staging of Alzheimer’s disease: past, present, and future perspectives. Trends in Molecular Medicine 28: 726-741.

Van Essen DC, Smith SM, Barch DM, Behrens TEJ, Yacoub E, Ugurbil K (2013) The WU-Minn Human Connectome Project: An overview. NeuroImage 80: 62-79.

Veitch DP, Weiner MW, Aisen PS, Beckett LA, Cairns NJ, Green RC, Harvey D, Jack Jr CR, Jagust W, Morris JC, Petersen RC, Saykin AJ, Shaw LM, Toga AW, Trojanowski JQ, Alzheimer's Disease Neuroimaging I (2019) Understanding disease progression and improving Alzheimer's disease clinical trials: Recent highlights from the Alzheimer's Disease Neuroimaging Initiative. Alzheimer's & Dementia 15: 106-152.

Wechsler D (1987) Wechsler Memory Scale-Revised Manual. The Psychological Corporation, San Antonio, TX

Weintraub S, Besser L, Dodge HH, Teylan M, Ferris S, Goldstein FC, Giordani B, Kramer J, Loewenstein D, Marson D, Mungas D, Salmon D, Welsh-Bohmer K, Zhou X-H, Shirk SD, Atri A, Kukull WA, Phelps C, Morris JC (2018) Version 3 of the Alzheimer Disease Centers’ Neuropsychological Test Battery in the Uniform Data Set (UDS). Alzheimer Disease & Associated Disorders 32.

533 Yeo BT, Krienen FM, Sepulcre J, Sabuncu MR, Lashkari D, Hollinshead M, Roffman JL, Smoller JW, Zöllei L, Polimeni JR,
534 Fischl B, Liu H, Buckner RL (2011) The organization of the human cerebral cortex estimated by intrinsic functional
535 connectivity. Journal of Neurophysiology 106: 1125-1165.
536 Zalesky A, Fornito A, Bullmore ET (2010) Network-based statistic: Identifying differences in brain networks. NeuroImage
537 53: 1197-1207.
538 Zamani Esfahlani F, Byrge L, Tanner J, Sporns O, Kennedy DP, Betzel RF (2022) Edge-centric analysis of time-varying
539 functional brain networks with applications in autism spectrum disorder. NeuroImage 263: 119591.
540 Zamani Esfahlani F, Jo Y, Faskowitz J, Byrge L, Kennedy DP, Sporns O, Betzel RF (2020) High-amplitude cofluctuations in
541 cortical activity drive functional connectivity. Proceedings of the National Academy of Sciences 117: 28393.
542 Zhang Z, Zheng H, Liang K, Wang H, Kong S, Hu J, Wu F, Sun G (2015) Functional degeneration in dorsal and ventral
543 attention systems in amnestic mild cognitive impairment and Alzheimer's disease: An fMRI study. Neuroscience
544 letters 585: 160-165.

545